axis to be perpendicular to the substrate surface. Unfortunately, it is not possible to be more definitive at this time. Future experiments will be directed toward explaining these observations.

Finally, one cannot ignore that the polymer–substrate interfacial fold plane in fold-plane epitaxy may be an example of an adjacent reentry chain fold. Thus, our work may be relevant to the issue of adjacent vs. nonadjacent reentry of chain-folded polymer single crystals.[14-17] Conceptually, the very nature of epitaxial crystallization, requiring that a crystalline polymer plane interact with a crystalline surface to produce the observed regular orientations, would lead one to envision a highly ordered, if not crystalline interfacial fold-plane surface for fold-plane epitaxial crystals. This intuitive feeling is further supported by the potential lattice matching between the substrate surface and the *ab* plane of the polymer crystal. A crystalline interfacial fold plane seems to be a quite probable state. However, nonadjacent reentry chain segments, which run parallel to the substrate surface along the directions observed for POM in Figure 1 and which likely have lengths which are integral multiples of the fold-plane separation distances, before reentering the polymer crystal, are also possible. Clearly, however, tie chains, fold loops of arbitrary size, and random chain reentry into the same polymer crystal, with respect to a frame of reference at the interface, are quite unlikely for the interfacial layer of polymer.

These preliminary investigations cannot resolve, nor were they originally intended to resolve, the question of adjacent vs. nonadjacent reentry. However, fold-plane epitaxial studies may be helpful in the investigation of this issue. We have shown, through morphological observations and electron diffraction, that fold-plane epitaxial crystallization of POM does occur from concentrated solutions onto (001) cleavage planes of mica. Ongoing and future experiments will deal with the mechanism of fold-plane epitaxial growth, as well as with extensions to other polymers and substrates.

Acknowledgment. We gratefully acknowledge the support of this work by the National Science Foundation (Grant No. ENG 78-24007).

References and Notes

(1) J. Willems, *Discuss. Faraday Soc.*, **25**, 204 (1957).
(2) E. W. Fischer, *Kolloid-Z.*, **159**, 108 (1958).
(3) J. A. Koutsky, A. G. Walton, and E. Baer, *J. Polym. Sci., Part A-2*, **4**, 611 (1966).
(4) S. Wellinghoff, F. Rybnikar, and E. Baer, *J. Macromol. Sci., Polym. Phys. Ed.*, **B10**, 1 (1974).
(5) S. E. Rickert and E. Baer, *J. Appl. Phys.*, **47**, 4304 (1976).
(6) C. M. Balik, R. Farmer, and E. Baer, *J. Mater. Sci.*, **14**, 1511 (1979).
(7) C. M. Balik and A. J. Hopfinger, *J. Polym. Sci., Polym. Phys. Ed.*, **16**, 1897 (1978).
(8) F. Tuinstra and E. Baer, *J. Polym. Sci., Polym. Lett. Ed.*, **8**, 861 (1970).
(9) K. Kobayashi and T. Takahashi, *Kagaku (Tokyo)*, **34**, 325 (1964).
(10) J. A. Koutsky, A. Walton, and E. Baer, *J. Polym. Sci., Polym. Lett. Ed.*, **B5**, 177 (1967).
(11) E. Suito and M. Nakahira in "Electron-Optical Investigations of Clays", J. A. Gard, Ed., Alden Press, Oxford, 1971, p 231.
(12) L. Bragg, G. F. Claringbull, and W. H. Taylor in "Crystal Structures of Minerals", Cornell University Press, Ithaca, NY, 1965.
(13) G. A. Carazzolo, *J. Polym. Sci., Part A*, 1, 1573 (1963).
(14) J. I. Lauritzen, Jr., and J. D. Hoffman, *J. Res. Natl. Bur. Stand., Sect. A*, **64A**, 73 (1960).
(15) P. H. Geil in "Polymer Single Crystals", Robert E. Krieger Publishing Co., Huntington, NY, 1963.
(16) P. J. Flory, *J. Am. Chem. Soc.*, **84**, 2857 (1962).
(17) P. J. Flory and D. Y. Yoon, *Nature (London)*, **272**, 226 (1978).

Elastic Properties of Well-Characterized Ethylene–Propylene Copolymer Networks

Dale S. Pearson*,† and William W. Graessley*

Materials Science and Engineering Department, Northwestern University, Evanston, Illinois 60201. *Received January 25, 1980*

ABSTRACT: A series of networks were prepared by cross-linking well-characterized ethylene–propylene copolymers with high-energy electron radiation. The cross-link density and other structural features of the networks were determined by analyzing the rate of increase of gel content with radiation dose. Stress–strain measurements revealed that the elastic modulus was considerably greater than that predicted by the classical theories of rubber elasticity. The initial modulus, however, could be calculated by assuming it to be the sum of two parts, one a chemical contribution proportional to the number of strands in the network and the other a topological contribution from entanglements trapped in the network by the cross-linking process. The value obtained for G_e^{max}, the maximum entanglement contribution to the equilibrium modulus, was equal within experimental error to G_N^0, the plateau modulus obtained from dynamic measurements on the un-cross-linked polymer.

Rubber elasticity is one of the classical problems of polymer physics. The essential goal is to develop a theory for relating the mechanical properties of rubber networks to their molecular structure. Early attempts in this direction assumed that the force required to deform the rubber arises entirely within the strands which connect the junctions in the network. Interactions between neighboring strands were ignored insofar as the strain-dependent properties were concerned. The principal result of this approach was the prediction that the shear modulus is approximately equal to the number density of strands in the network multiplied by kT[1] (eq 1).

$$G \simeq \nu kT \tag{1}$$

When rubber networks are formed from concentrated solutions or melts, the domains occupied by neighboring strands will overlap to a considerable extent.[2] Since the strands cannot pass through each other, molecular rearrangements which occur upon deformation may be influ-

† Present address: Bell Laboratories, Murray Hill, NJ 07974.

0024-9297/80/2213-1001$01.00/0

enced by interactions of a topological nature. Such constraints are expected to increase the shear modulus above that predicted by eq 1.[3]

Measurements on rubber networks prepared from polybutadiene have shown that the shear modulus can be substantially larger than νkT.[4] Furthermore, the results of that study are consistent with the idea that topological interactions (entanglements) between network strands are responsible for the increased modulus. The potential entanglement contribution, as judged by the magnitude of the plateau modulus, is considerably smaller in the case of poly(dimethylsiloxane). Indeed, there is some controversy currently about whether one needs to consider entanglement contributions in the equilibrium elastic properties of poly(dimethylsiloxane) networks.[5-8] In this paper we present data on well-characterized networks formed from ethylene–propylene copolymers which support the need to consider entanglement contributions. In fact, for the networks studied here the dominant part of the modulus is contributed by topological interactions.

The Shear Modulus of a Rubber Network

Theories of rubber elasticity which neglect interaction between network strands are called "phantom" network theories, a name suggestive of strands which are free to pass through each other's contour. The calculated shear modulus of such a network is[9,10]

$$G = (\nu - \mu)kT \tag{2}$$

where ν and μ are the number densities of elastically active strands and junctions. A junction is elastically active if at least three paths leading away from it are independently attached to the network; a strand is elastically active if it is bounded at each end by elastically active junctions.[11,12] For a perfect tetrafunctional network there are twice as many strands as junctions and eq 2 reduces to

$$G = \tfrac{1}{2}\nu kT \tag{3}$$

In phantom rubber networks the junctions fluctuate about their mean positions. The extent of fluctuations is governed only by the number of strands connected to the junction. One effect of topological interactions in a real rubber network might be to reduce the magnitude of these fluctuations. Theories have been developed along these lines[13,14] and they predict that if entanglements restrict junction fluctuations entirely, then the shear modulus would increase to

$$G = \nu kT \tag{4}$$

The modulus for a network whose behavior is intermediate to the extremes could be described empirically by[4]

$$G = (\nu - h\mu)kT \tag{5}$$

where h is a parameter between 0 and 1.

Equation 5 would apply to a rubber network for which the only effect of entanglements is to reduce junction fluctuations. However, if interactions between strands elsewhere along their contours are important, a different approach is required. We describe a method similar to that proposed by Langley.[15] When a high molecular weight un-cross-linked polymer is tested under dynamic conditions, the shear modulus has an essentially constant value, G_N^0, over a wide range of frequency. This behavior is consistent with the concept that a temporary entangled network is present with a lifetime that is longer than the experimental time scale. If a portion of this network becomes permanently fixed or trapped by the addition of cross-links, then the modulus should be greater than a phantom network having the same structure. Assuming the entanglement effect is simply additive, the shear modulus, G, would be the sum of two parts: a chemical contribution from the strands which join the junctions, G_c, and a topological contribution from the permanently entangled chains, G_e.

$$G = G_c + G_e \tag{6}$$

We assume that the topological contribution is the product of G_e^{max}, the maximum possible contribution of entangled chains to the modulus, and T_e, the fraction of this maximum actually obtained (eq 7). If we further

$$G_e = T_e G_e^{max} \tag{7}$$

assume that the chemical contribution is that given by eq 5, then the shear modulus is

$$G = (\nu - h\mu)kT + T_e G_e^{max} \tag{8}$$

Langley has suggested that T_e should be equal to the probability that all four paths leading away from two interacting chains are connected to the continuous structure of the network.[15] This is equivalent to the probability that any pair of interacting units are each part of elastically active strands and are thereby part of closed loops in the network.[16] We want to emphasize that our view of the topological effects that contribute to the modulus is one of pairwise interactions between network chains. However, we do not view these interactions as being highly localized ones like those of a cross-link.

Equations 6, 7, and 8 provide a link between the modulus of a rubber network and its molecular structure. The parameter G_e^{max} is expected to be closely related to G_N^0, the plateau modulus of the un-cross-linked polymer. The relationship between G_N^0 and molecular structure is still somewhat uncertain.[17,18] The parameter h is difficult to establish theoretically, but for highly entangled networks it should be near 1.[14]

To test these ideas we have prepared rubber networks with known values of ν, μ, and T_e and then measured their moduli under equilibrium conditions. The methods for doing this and our results are given in the following sections.

Experimental Section

Polymer Preparation and Characterization. The polymers used in this study are copolymers of ethylene and propylene obtained from Dr. G. Ver Strate of the Exxon Chemical Co. The starting polymer contained 0.6 mol fraction ethylene and was polymerized under conditions which were expected to give amorphous, linear materials. Differential scanning calorimetry, X-ray, and density measurements all indicated that the melting point was below room temperature. It was fractionated by sequential precipitation from cyclohexane with isopropyl alcohol. Nine fractions were obtained but those with the two highest molecular weights and the lowest molecular weight were not used. The molecular weight distributions of the remaining fractions were determined by gel permeation chromatography (Waters GPC Model 200) in THF. A molecular weight vs. elution volume calibration was established with polystyrene standards[19] and then applied to EP copolymers using the universal calibration method of Benoit[20] and the Mark–Houwink equation reported by Smith[21]

$$[\eta]_{THF} = 3.88 \times 10^{-4} M^{0.686} \tag{9}$$

The GPC Model 200 was also equipped with an on-line viscometer which was used as described elsewhere[22] to confirm the expected linear nature of the samples.

Ver Strate[23] determined the intrinsic viscosities of all samples in decalin at 135 °C and $\bar{M}_w$ of sample EP 208 by low-angle laser light scattering (LALLS) in trichlorobenzene at 135 °C. The intrinsic viscosity data were used to estimate $\bar{M}_w$ from the Mark–Houwink equation established by Ver Strate[24] with LALLS (eq 10). The molecular weight distribution and composition of

$$[\eta]_{Dec} = 2.47 \times 10^{-4} \bar{M}_w^{0.759} \tag{10}$$

Table I
Molecular Characterization Data

sample	M_w (GPC) × 10^{-3}	M_n (GPC) × 10^{-3}	M_w/M_n	$[\eta]_{dec}$, dL/g	M_w ($[\eta]$) × 10^{-3}
EP 090	90	52	1.73	1.37	87
EP 107	107	65	1.64	1.58	106
EP 133	133	91	1.46	1.94	139
EP 162	162	110	1.47	2.46	190
EP 208	208[a]	129	1.61	2.88	233
EP 310	310	153	2.03	3.92	350

[a] M_w for EP 208 is 198 × 10^3 by low-angle laser light scattering in TCB at 135 °C.

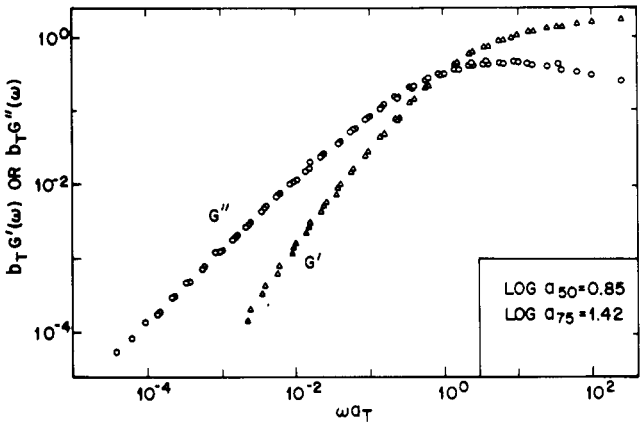

Figure 1. The storage and loss moduli as a function of frequency reduced to 25 °C for sample EP 107.

the fractions used by Ver Strate were similar to those of the samples in this study.

Good agreement was obtained between the various measurements of molecular weight. A summary of the results is given in Table I.

Rheological Measurements. The linear viscoelastic properties of samples EP 107 and EP 208 were measured with a Rheometrics mechanical spectrometer. Values of the storage and loss moduli, $G'(\omega)$ and $G''(\omega)$, were determined as functions of frequency, ω, and temperature using the eccentric-rotating-disk method. Samples 1 mm thick × 2.5 mm in diameter were tested from 0.001 to 100 rad/s and strain amplitude up to 0.2. At the higher frequencies where the measured forces were large it was necessary to correct the strain amplitude for instrumental compliance. The procedure for doing this has been described by Raju et al.[25]

Data gathered at 25, 50, and 75 °C were reduced to a common temperature of 25 °C by first correcting the moduli by a vertical shift factor, $b_T = T_0\rho_0/T\rho$, and then shifting along the frequency scale until superposition was obtained.[26] The required horizontal shift factors, a_T, were essentially the same as those determined by Ferry and co-workers[27] on a similar copolymer (see Figure 1). The plateau modulus, G_N^0, was obtained by using[26] eq 11, where

$$G_N^0 = \frac{2}{\pi}\int_{-\infty}^{\infty}[G''(\omega) - G_S''(\omega)]\ d\ \ln\ \omega \qquad (11)$$

$G''(\omega)$ is the dynamic loss modulus and $G_S''(\omega)$ is the contribution to the loss modulus from the transition region. The values of G_N^0 so obtained were 1.88 MPa for EP 107 and 1.60 MPa for EP 208. These values are somewhat higher than the value of 1.26 MPa obtained by integrating the loss-compliance spectra of a similar copolymer.[27]

Network Formation and Characterization. The small amount of antioxidant added to the samples during the fractionation procedure was removed just prior to cross-linking by dissolving them in cyclohexane and precipitating in methanol. The polymers were thoroughly dried in vacuo and then molded at 50 °C between sheets of Mylar into rectangular strips 25 × 50 × 1 mm. Molding was done at least 1 week before cross-linking to allow sufficient time for the samples to relax to an isotropic state. The viscoelastic measurements described above indicated that the time required for the highest molecular weight sample to relax was about one-half day at room temperature.

The samples were cross-linked by high-energy electron radiation (1.3 MeV). An electron beam generator (Dynamitron) suitable for this procedure was made available by Dr. Georg Böhm at the Firestone Tire and Rubber Co. The dose was delivered to the samples in increments of 0.25–2 Mrd by repeatedly passing them through a scanned electron beam. Sufficient waiting periods between passes were allowed to avoid heating the samples more than 25 °C above room temperature.

At this electron energy (1.3 MeV) the radiation dose increases almost linearly with sample thickness up to 2.5 mm.[28] A uniform exposure could therefore be achieved by delivering half of the dose to each side of the sample. The dose was measured by monitoring the change in optical density of the cellophane tape placed on the surface of the samples.

The gel content was determined by extraction with cyclohexane. Weighed pieces of polymer (approx 0.1 g) were placed in 100 mL of solvent containing 0.1% antioxidant. After 5 weeks the solvent was decanted and replaced with pure cyclohexane. After another week the swollen gels were removed, weighed, and then dried to a constant weight under vacuum. The swelling behavior will be discussed in a future publication.

Elastic Measurements. Antioxidant (Ionol) was added to the networks by first swelling them to approximately twice their initial volume in a cyclohexane solution containing 0.2% antioxidant and then drying in vacuo to a constant weight. Strips 6.5 mm wide by 50 mm long were cut with a steel die and then marked along each edge with six or seven ink dots. The separation of the dots and the cross-sectional area of each strip was measured with a Gaertner cathetometer (Model 940-303P) having a reported precision of 1 μm.

After the rest dimensions were determined, the samples were mounted in lightweight grips, the lower grips being equipped with a hook for holding weights. A load was applied and the strain was measured at periodic intervals until the sample was judged to be at equilibrium (see below). The amount of weight was then increased or decreased and a new equilibrium point was established. Data obtained during loading and unloading cycles showed no significant hysteresis effects.

The time required to reach equilibrium was a function of cross-link density. For samples with more than ~500 main-chain carbon atoms between network junctions, equilibrium was not attained after 30 days and the test was stopped. Samples with less than ~300 carbon atoms between junctions attained equilibrium in less than 2 days. The number of carbon atoms between junctions and the average time required to reach equilibrium are given in Table II. For a number of samples the load was left on for periods of 25–60 days after it was judged that an equilibrium length had been attained. No additional change was noted.

In one case a sample that came to equilibrium at room temperature was retested at elevated temperatures (up to 100 °C) by hanging the sample inside a thermostated chamber equipped with a polycarbonate window for viewing the dots (see below). The equilibrium stress–strain values were used to calculate a reduced stress, $\sigma/(\lambda - 1/\lambda^2)$, where σ is the force, f, divided by the initial cross-sectional area, A_0, and λ is the ratio of the deformed length to the rest length, L/L_0. These data, when plotted on a Mooney–Rivlin plot (Figure 2) of $\sigma/(\lambda - 1/\lambda^2)$ vs. $1/\lambda$, fall on relatively straight lines over the entire range of strain studied ($1.05 < \lambda < 1.3$). For some samples the line showed a slight upward or downward curvature at low strains, which might be due to an error in the measurement of the rest length.[29] The slope of the lines, $2C_2$, and their intercept at zero strain, $G = 2C_1 + 2C_2$, are listed in Table II.

Analysis of Gel Curve Data

A method for calculating the concentration of cross-linked and fractured units from the gelation behavior has been given by Pearson and Graessley.[16] It relies on the assumption that cross-links and scissions are randomly distributed. Detailed arguments supporting this assumption are given in Appendix A.

For long primary chains the relationship between the gel fraction, g, and the fractions of units which are tetra-

Table II
Network Characterization Data

sample	D, Mrd	t_e,[a] days	G, MPa	$2C_1$, MPa	$2C_2$, MPa	νkT, MPa	T_e	$2\nu/\mu$[b]	$\bar{L}$[c]
EP 090	77.5	2	0.67			0.234	0.276	3.40	286
EP 090	210.8	2	0.80			0.337	0.306	3.42	210
EP 133	53.7	10	0.64	0.46	0.18	0.179	0.283	3.40	378
EP 133	66.3	3	0.69	0.50	0.19	0.227	0.300	3.41	308
EP 133	85.6	2	0.83	0.60	0.23	0.302	0.317	3.43	238
EP 133	106.5	2	0.93	0.70	0.23	0.382	0.329	3.44	192
EP 162	61.6	2	0.73	0.45	0.28	0.203	0.309	3.42	350
EP 162	82.4	2	0.85	0.58	0.27	0.279	0.328	3.44	262
EP 162	102.1	2	0.95	0.60	0.35	0.351	0.339	3.45	212
EP 208	49.8	3	0.70	0.49	0.21	0.158	0.324	3.43	458
EP 208	61.7	2	0.74	0.58	0.16	0.201	0.340	3.45	370
EP 208	74.0	2	0.88	0.53	0.35	0.245	0.352	3.45	308
EP 208	82.6	2	0.90	0.59	0.31	0.275	0.358	3.46	276
EP 208	103.9	2	0.98	0.67	0.31	0.351	0.369	3.47	220
EP 310	62.5	2	0.82	0.55	0.27	0.208	0.376	3.47	376
EP 310	74.4	2	0.89	0.58	0.31	0.250	0.386	3.48	316
EP 310	87.4	2	0.96	0.71	0.25	0.297	0.394	3.49	270
EP 310	102.6	2	1.05	0.67	0.38	0.351	0.401	3.49	230

[a] Average time to reach equilibrium per load. [b] Average number of elastically active strands per elastically active junction. [c] Average number of carbon atoms per elastically active strand. See eq 35, ref 16.

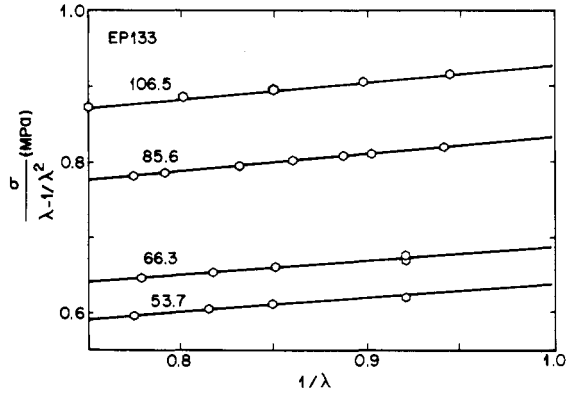

Figure 2. Mooney–Rivlin plots for cross-linked samples of EP 133. Numbers on each line indicate radiation dose in megarads.

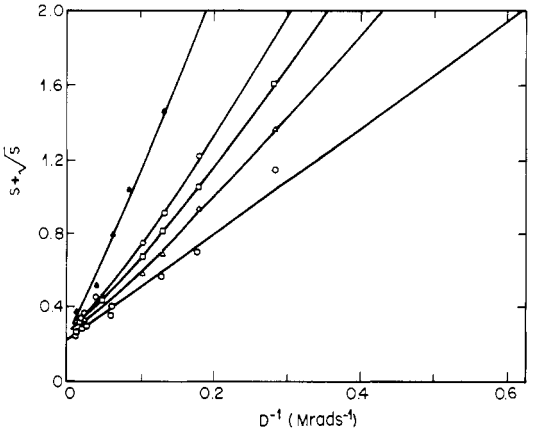

Figure 3. Charlesby–Pinner plots for samples EP 310 (○), EP 208 (△), EP 162 (□), EP 133 (○), and EP 090 (▲).

functionally cross-linked, α, and which are fractured, β, is given by

$$g = \sum_{r=1}^{\infty} W_r \left\{ 2\lambda \left[\frac{(1-\zeta)^r}{r\zeta} \right] - \lambda^2 \left[1 - \frac{2-2(1-\zeta)^r}{r\zeta} + (1-\zeta)^r \right] \right\} \quad (12)$$

where W_r is the weight fraction of primary chains having r units, $\zeta = \beta + \alpha g$ and $\lambda = \alpha g/\zeta$. The results from gel permeation chromatography[29] indicate that the molecular weight distributions can be approximated by the Schulz–Zimm distribution[30]

$$W_r = [b^b/\bar{r}_n\Gamma(b)](r/\bar{r}_n)^b \exp(-br/\bar{r}_n) \quad (13)$$

where $\bar{r}_n$ and $\bar{r}_w$ are the number and weight average degree of polymerization, $b = \bar{r}_n/(\bar{r}_w - \bar{r}_n)$, and $\Gamma(\cdot)$ is the gamma function. When this distribution is substituted into eq 12 and the summation completed, expression 14 for g is obtained, where $\gamma = \alpha\bar{r}_n$ and $\xi = \beta/\alpha + g$. We assume that the rate of cross-linking and scission are directly proportional to the radiation dose, D.

$$g = 2\lambda \left[1 - \frac{1-(1+\gamma\xi/b)^{-b}}{\gamma\xi} \right] - \lambda^2 \left[1 - \frac{2-2(1+\gamma\xi/b)^{-b}}{\gamma\xi} + (1+\gamma\xi/b)^{-b-1} \right] \quad (14)$$

$$\alpha = \alpha_0 D \qquad \beta = \beta_0 D \quad (15)$$

At high doses, g approaches the maximum value

$$\lim_{D\to\infty} g = g_{max} = \frac{1}{2}\left[1 - 2\frac{\beta}{\alpha} + \left(1 + 4\frac{\beta}{\alpha} \right)^{1/2} \right] \quad (16)$$

or equivalently the sol fraction approaches the minimum value

$$s_{min} + s_{min}^{1/2} = \beta/\alpha \quad (17)$$

Equation 17 is the basis for the Charlesby–Pinner plot[31] on which $s + s^{1/2}$ is plotted vs. the reciprocal dose and then extrapolated to obtain the cross-link to scission ratio, β/α. Figure 3 shows the gelation data plotted in this manner. The value of β/α obtained by extrapolation is essentially the same for all polymers (0.25). The gel data were further analyzed by a nonlinear regression analysis that minimized the sum of squares between the experimental gel fraction and the value calculated with eq 14. Slight differences were noted in the magnitude of α_0 and β_0 determined for each fraction (see Table III). Some of this variation is probably due to experimental errors in the molecular weights.

Table III
Radiation Constants for Cross-Linking and Scission

sample	$\alpha_0 \times 10^5$, Mrd^{-1}	$\beta_0 \times 10^5$, Mrd^{-1}	α_0/β_0
EP 090	1.94	7.99	0.24
EP 133	2.27	8.71	0.26
EP 162	2.11	8.24	0.26
EP 208	1.84	7.77	0.24
EP 310	1.65	7.50	0.22

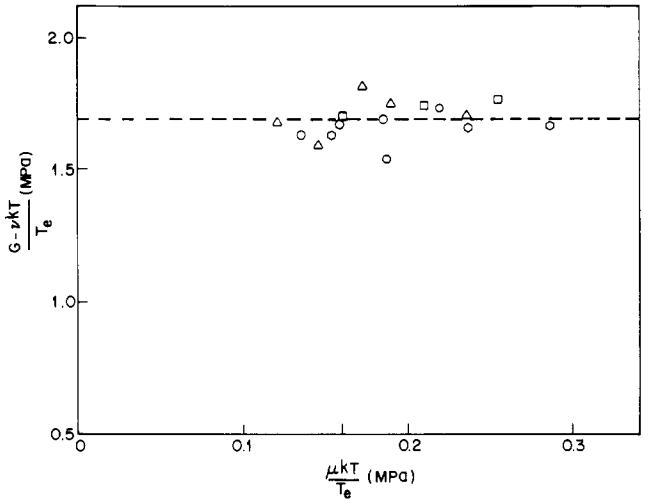

Figure 4. Plot of $(G - \nu kT)/T_e$ vs. $\mu kT/T_e$ used to estimate the parameter h. Symbols are the same as for Figure 3.

The procedure used to calculate α_0 and β_0 is not complicated, but practical considerations require using a digital computer. A somewhat simpler method for calculating α_0, β_0, and the structural parameters of the network based entirely on graphical means is discussed in Appendix B.

Calculation of Network Parameters

Pearson and Graessley[16] have given expressions for calculating the network parameters ν, μ, and T_e (eq 18–22),

$$\nu = \tfrac{1}{2}c\gamma(3p_1p_2 + 2p_2^2) \tag{18}$$

$$\mu = \tfrac{1}{2}c\gamma(2p_1p_2 + p_2^2) \tag{19}$$

$$T_e = p_2^2 \tag{20}$$

$$p_1 = g - p_2 \tag{21}$$

$$p_2 = \lambda^2\left[1 - \frac{2 - 2(1 + \gamma\xi/b)^{-b}}{\gamma\xi} + (1 + \gamma\xi/b)^{-b-1}\right] \tag{22}$$

where c is the number density of polymer chains, p_1 is the probability that a randomly chosen un-cross-linked unit is connected to the gel along only one of the two paths leading away from it, and p_2 is the probability that it is connected along both paths. In applying these formulas we used the values of g calculated with eq 14 and the values of α_0 and β_0 given in Table III.

Values of νkT, $2\nu/\mu$ (the average functionality of a junction), and T_e were calculated with eq 18–21 at T = 298 K. The results are given in Table II.

Initial Modulus

Samples Tested at Room Temperature. Equation 8 suggests that values of $(G - \nu kT)/T_e$ plotted vs. $\mu kT/T_e$ should fall on a straight line with a slope of $-h$ and an intercept of G_e^{max}. Data for all of the networks tested are plotted in this manner in Figure 4. The results are scattered but they appear to fall on a line of zero slope, suggesting $h = 0$ and $G_e^{max} \simeq 1.7$ MPa. In Figure 5 the same data is plotted as G/T_e vs. $\nu kT/T_e$. The slope of this line is 1.11 which, within experimental error, is equal to the expected value of $1 - h\mu/\nu$ for $h = 0$. The intercept of 1.60 MPa is close to the average value of G_N^0 determined for the polymers prior to cross-linking (1.72 MPa). These findings show that entangling interactions can strongly influence the equilibrium elastic properties if the plateau modulus is large. Both interchain interactions and the suppression of junction fluctuations have increased the modulus substantially above that expected for a phantom network. The initial modulus, G, is plotted as a function of radiation dose in Figure 6. The curves passing through the data were calculated with eq 8 with $h = 0$ and G_e^{max} = 1.60 MPa. The essentially straight lines near the bottom of the figure show where the experimental data would fall if the only effect of entanglements was to suppress junction fluctuations ($h = 0$, $G_e^{max} = 0$). Trapped entanglements clearly play a major role in determining the magnitude of the initial modulus.

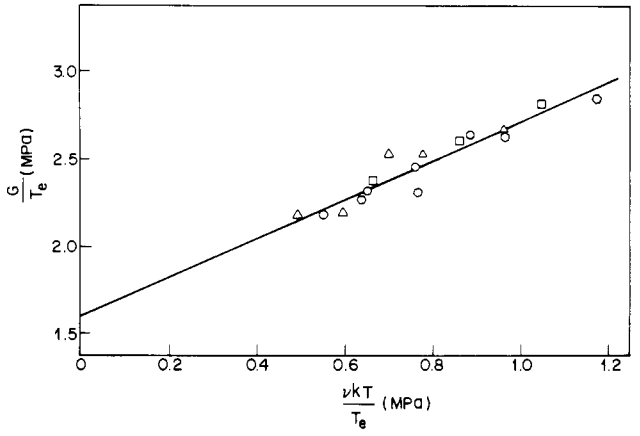

Figure 5. Plot of G/T_e vs. $\nu kT/T_e$ used to estimate the parameter G_e^{max} (Langley plot). Symbols are the same as for Figure 3.

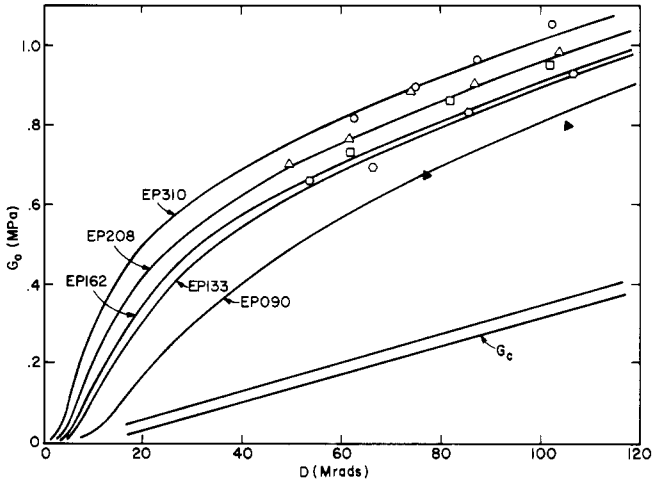

Figure 6. Shear modulus of all samples as a function of radiation dose. The curves were calculated with $h = 0$ and G_e^{max} = 1.60 MPa. The straight line indicates where data would fall if the only effect of entanglements was to reduce junction fluctuations. Upper line is for sample EP 310 and lower line for sample EP 090.

Samples Tested at Elevated Temperature. Sample EP 208 (82.6 Mrd) was tested at elevated temperatures to ensure that processes outside the scope of present theories were not affecting the modulus. For example, if trace amounts of crystallinity were present and acted as additional cross-links, then raising the temperature would melt this material and the modulus would decrease.

Table IV
Modulus of EP 208 (82.6 Mrd) at Elevated Temperature[a]

T, °C	G_T, MPa	G_T/G_{25} exptl	G_T/G_{25} calcd (eq 23)
25	0.895	1.00	1.00
66	1.10	1.23	1.19
98.5	1.24	1.38	1.37

[a] Based on the measured value of 6.6×10^{-4}/°C for $(1/V)\,dV/dT$ and the average value of 1.4×10^{-3}/°C for $(1/\langle r^2\rangle^0)\,d\langle r^2\rangle^0/dT$ obtained from several thermoelastic studies,[33-36] a dilute-solution viscosity study,[37] and rotational isomeric state calculations.[38]

We found that the modulus increased with temperature over the entire range studied (25–100 °C). Lacking a constitutive equation for entangled rubber networks, we compared our results with the predictions for a phantom rubber network. According to this theory, the ratio of the modulus at two different temperatures should be equal to[32]

$$\frac{G_1}{G_2} = \frac{V_2 T_1 \langle r^2\rangle_2{}^0 \langle r^2\rangle_1}{V_1 T_2 \langle r^2\rangle_1{}^0 \langle r^2\rangle_2} \tag{23}$$

where the subscript refers to the temperature, V_i is the volume of the network, $\langle r^2\rangle_i$ is the mean square end-to-end vector of the chains in the network, and $\langle r^2\rangle_i{}^0$ is the mean square end-to-end vector of the chains in the network if they were free of the junction constraints. We assumed that V_i and $\langle r^2\rangle_i$ change with temperature in accordance with the thermal expansion coefficient of the network, $(1/V)\,dV/dT$, and that $\langle r^2\rangle_i{}^0$ change in accordance with experimental values of the temperature coefficient for chain dimensions, $(1/\langle r^2\rangle^0)\,d\langle r^2\rangle^0/dT$.[33-38] In Table IV we have listed the initial modulus obtained at three different temperatures. Also given is the ratio of the modulus at elevated temperature to the room-temperature modulus as determined experimentally and as calculated by eq 23. The ratios obtained by the two methods agree quite well. The results indicate a lack of crystallinity in our polymers, since the melting point is below room temperature and the calculated melting point elevation for the small strains employed is only on the order of 5 °C.[39] The limited precision and quantity of data prevented us from determining the separate temperature dependence of $2C_1$ and $2C_2$.

Finite Deformation Behavior

Much effort has been spent to find a molecular explanation for the departure of stress–strain data from neo-Hookean behavior.[40] In uniaxial tension this departure can easily be detected by a nonzero slope in a plot of $\sigma/(\lambda - 1/\lambda^2)$ vs. $1/\lambda$. Many investigators have suggested that if this plot is extrapolated to infinite strain, the intercept, $2C_1$, should be identified with the chemical network contribution, G_c. In Figure 7 we have plotted $2C_1$ vs. the calculated value of $G_c = \nu kT$. All of the values substantially exceed G_c, suggesting that $2C_1$ also contains a topological contribution.

In two recent experimental studies, Ferry and Kan[41] and Dossin and Graessley[4] have found a correlation between $2C_2$ and the topological contribution, $T_e G_e{}^{max}$. Their results can be cast in the form

$$\frac{2C_2}{2C_1 + 2C_2} = A + B\frac{T_e G_e{}^{max}}{T_e G_e{}^{max} + G_c} \tag{24}$$

A similar relation for $2C_1$ follows

$$2C_1 = (1 - A)G_c + (1 - A - B)G_e T_e{}^{max} \tag{25}$$

Ferry and Kan find $B \simeq 1$ and $A \simeq -0.275$. Dossin and Graessley find $B \simeq 0.5$ and $A \simeq 0$. Unfortunately, our data cover a very narrow range of $T_e G_e{}^{max}$ ($\sim$0.45–0.65) and hence we cannot judge which prediction is correct. In Figure 8 we have plotted the data according to eq 25 and drawn in the equations of Ferry–Kan and Dossin–Graessley. The data cluster near the intersection of the two lines. The scatter is probably due to small errors made in the rest-length measurement. Errors of this nature have a relatively small effect on the initial shear modulus, G, but a large effect on the separate values of $2C_1$ and $2C_2$.

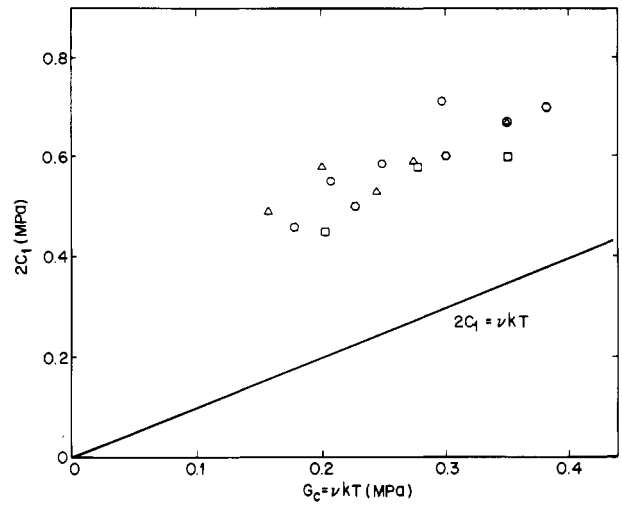

Figure 7. Mooney–Rivlin constant $2C_1$ as a function of the network chain density multiplied by kT, $G_c = \nu kT$. Straight line indicates the relationship $2C_1 = \nu kT$. Symbols are the same as for Figure 3.

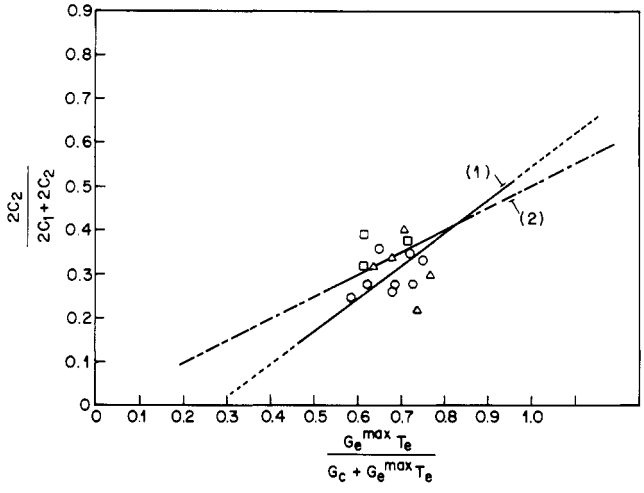

Figure 8. The ratio $2C_2/(2C_1 + 2C_2)$ as a function of $G_e{}^{max}T_e/(G_c + G_e{}^{max}T_e)$. Line 1 indicates the relationship of Ferry and Kan[41] and line 2 indicates the relationship of Dossin and Graessley.[4] Solid portions of line indicate range of experimental data used by these investigators. Symbols are the same as for Figure 3.

Conclusions and Discussion

We find that the initial shear modulus G in a series of 18 ethylene–propylene copolymer cross-linked networks can be expressed as the sum of two contributions, G_c from the chemical structure of the network, and $T_e G_e{}^{max}$ from the topological interactions. Within experimental error the chemical contribution is νkT, suggesting that the junction fluctuations are largely suppressed.[13,14] The topological contribution is large relative to the chemical contribution, $(G - \nu kT)/\nu kT$ ranging from 1.4–3.4. We find $G_e{}^{max} = 1.6$ MPa, in good agreement with the plateau modulus $G_N{}^0 = 1.7$ MPa obtained independently by dy-

namic measurements on the un-cross-linked polymer. Thus we conclude that the entanglement interactions responsible for the plateau in linear viscoelastic response are also the source of the topological contributions in equilibrium network elasticity. Finally, contrary to numerous suggestions in the literature, we find that $2C_1$ of the Mooney–Rivlin equation is not equal to the chemical contribution alone but can contain a sizable topological contribution as well.

These conclusions are virtually the same as those deduced from a recent study of polybutadiene cross-linked networks.[4] They differ slightly from results on poly(dimethylsiloxane) cross-linked networks by Langley and Polmanteer[5] and end-linked networks by Macosko and Valles.[6] These workers indeed find a topological contribution in the range expected ($G_e^{max} \approx G_N^0 \approx 0.3$ MPa) but only partial suppression of network junction fluctuations ($G_c = (\nu - h\mu)kT$, with $h \neq 0$). Although calling for further study, the latter difference is not a serious one in our opinion and is perhaps related to the relatively high entanglement densities in the polybutadiene and ethylene–propylene copolymer networks, which may tend to suppress junction fluctuations more effectively.

Of greater concern is the apparent conflict with extensive results on poly(dimethylsiloxane) end-linked networks reported by Mark and co-workers.[7,8] They find no need to include a topological contribution and obtain $G \approx \nu kT$, where ν is calculated assuming complete reaction. We believe, however, that even these results can be explained within a framework that includes entanglement trapping. The relative importance of chemical and topological contributions must, of course, depend on the relative magnitudes of $(\nu - h\mu)kT$ and $T_eG_N^0$. In completely reacted stoichiometric end-linked networks $T_e = 1$, and ν and μ can be calculated simply from reactant molecular weights and functionalities. However, these parameters are extremely sensitive to the extent of reaction. For example, at 90% conversion ν is only 72% of theoretical, and T_e is 0.64 in tetrafunctional networks.[6,29] At 80% conversion ν is 39% of theoretical, and T_e is 0.31. The calculated sol fractions at these conversions are 0.011 and 0.063, respectively. The extractable fractions reported by Mark and co-workers lie in the range 0.012–0.06.[7,8] If this material reflects unreacted polymer, substantial reductions in ν from theoretical values and relatively low trapping factors should be expected for those networks. Sensitivity to conversion is even greater in trifunctional networks. Thus the data on those end-linked networks may require some correction before being used to decide the question of topological contributions.

Acknowledgment. The authors are grateful to Dr. Gary Ver Strate of the Exxon Chemical Co. for providing and assisting in the characterization of the samples used in this study and for helpful discussions on interpreting the results, to Dr. Georg Böhm of the Firestone Tire and Rubber Co. for making the Firestone radiation facility available to us, to Dr. Mitio Inokuti of Argonne National Laboratory for discussions on the spatial distribution of cross-links in irradiated polymers, to Professor Chris Macosko for valuable suggestions on the manuscript, and to our colleague, Dr. Luc Dossin, for his help throughout this study. This work was supported by a grant from the Exxon Chemical Co. and by fellowships from Brunswick Corp. and the Cabell Fellowship Fund of Northwestern University. Use of the facilities of the Northwestern University Materials Research Center, supported by the National Science Foundation (Grant No. DMR 76-80847), is gratefully acknowledged.

Appendix A. Distribution of Cross-Links in Irradiated Polymers

The theory of gelation presented above assumes that the cross-linked units are randomly distributed. We have tried to verify this assumption both by considering what is known about the spatial distribution of events in radiation chemistry and by experimental comparisons.

When a high-energy electron traverses a sample, the initial effect is to ionize and excite polymer molecules; the cross-links are produced by later reactions which come after ion–electron recombination and deexcitation. Because the polymer is irradiated in the solid state, diffusion of the macroions which are formed is highly suppressed. Hence, the spatial distribution of the cross-links will be controlled by the initial distribution of the ions. The nature of this distribution is a relatively unexplored area and the discussion which follows is unfortunately only qualitative.

A high-energy electron traveling through a thin specimen proceeds along a relatively straight track. This primary electron is scattered by other electrons, and some of these interactions lead to the ejection of a secondary electron with the simultaneous creation of an ion. The distance between successive ions is controlled by the velocity of the electrons. Provided the primary electron is scattered many times as it traverses the sample, the mean electron energy at the end of the track can be estimated from[42]

$$\bar{T} = T_0 - (dT/dx)l \tag{A1}$$

where T_0 is the initial electron energy (in this case 1.3 MeV), dT/dx is the stopping power, and l is the sample thickness. For a sample 1-mm thick and with a stopping power of 1.928 (MeV·cm^2)/g determined for 1.3-MeV electrons in polyethylene, the average energy is only reduced by 13%. As a result of this small change in the initial electron energy, the average number of ionizations per unit track length will be essentially constant, and the total number of primary ionizations per electron can be estimated with

$$m_i = \sigma_i(T)n_0l \tag{A2}$$

where $\sigma_i(T)$ is the cross-section for primary ionization, and n_0 is the number density of the scattering groups. For a polymer composed of CH_2 groups and irradiated with 1.3-MeV electrons, σ_i is 9.4×10^{-19} cm^2 and m_i is ~3500 ionizations/mm.[42] This corresponds to a distance of ~3000 Å between primary ions. If the distribution of *primary* ions is to be considered random, the distance between tracks of the electrons must be smaller than the distance between successive ionizations along the tracks.

The average distance between neighboring tracks can be calculated from the electron flux at the surface (eq A3).

$$\phi = D/(dT/dx) \tag{A3}$$

In eq A3, ϕ is the flux in electrons/cm^2 and D is the dose at the surface in MeV/g. The average distance between tracks is

$$\bar{L} = 1/\phi^{1/2} \tag{A4}$$

From eq A3 and A4 the average spacing between the tracks of the primary electrons becomes equal to the ion spacing along the track at a dose of only 6000 rd. Because this dose is a small fraction of that given to the samples in this study, we have concluded that the distribution of primary ions is random.

What about the spatial distribution of the ions produced by the secondary electrons? Owing to the T^{-2} dependence

of the energy spectrum of these electrons,[44] a large fraction of them have energies so low they are not capable of further ionization. However, we can estimate the number of ionizations produced by secondary electrons as follows. From eq A2 and A3 it can be calculated that ~1.8 primary ions are produced per 100 eV of absorbed energy. Because the total yield of ions in irradiated hydrocarbons is known to be ~4/100 eV,[31] the ratio of secondary ions to primary ions is close to unity and hence, on the average, there will not be a large number of secondary ions clustered around primary ions. The probability of clusters of cross-links is even smaller because the yield of cross-links is only one for every 4 ions. Thus the distribution of cross-links, like that for primary ions, should be virtually random for doses above 10^4 rd.

The experimental evidence is as follows. At sufficiently low doses the cross-links in a polymer must be confined to clusters or spurs around the tracks of primary electrons. As the dose increases the clusters on neighboring tracks begin to overlap and eventually a random distribution will be obtained. It has been suggested that if the dose given to a sample is not sufficient to produce a random distribution of cross-links, the yield of gel will be reduced.[45] Such an effect could cause an incorrect counting of cross-links at high doses. However, this would also cause the shape of the gel curve for very high molecular weight polymers to be different from that for low molecular weight polymers because lower doses are required to gel the higher molecular weight materials. In the Graessley–Dossin work[4] polybutadienes having molecular weights from 22 000 to 750 000 were given doses in the 1–65 Mrd range. When the gel content of these polymers ($1 < D < 25$ Mrd) is plotted vs. the product of molecular weight and dose, all of the data superimpose onto a single master curve (see Figure 3 of ref 4). No systematic differences were found between high molecular weight (low dose) samples and low molecular weight (high dose) samples at the same gel fraction. This clearly supports the randomness assumption at all doses used and particularly throughout the range of doses (16–65 Mrd) used to prepare networks for mechanical measurements in that study. Similar results were obtained in a study of gel points in polystyrene samples with molecular weights from 56 000 to 3 400 000.[46] No significant departures from random cross-linking predictions (constancy of the product $\bar{M}_w D_g$) were found.

In the present study the range of molecular weights is considerably smaller. The product of gelation dose and molecular weight was found to be essentially constant in the range 1.5–5 Mrd, and no unusual departures in the gel curve shapes (4–100 Mrd) from expectation based on the random theory were found. We conclude that cross-linking is random throughout the range of doses used on samples for the mechanical measurements (50–100 Mrd).

Appendix B. A Graphical Method for Determining Cross-Linking and Scission Rates

The cross-linking and scission rates, α_0 and β_0, were determined by a nonlinear regression analysis. This procedure is not complicated, but practical considerations dictate the use of a digital computer. One of us has given a simpler method which requires only graphical manipulations.[47]

For molecular weight distributions which are not too different from the most probable distribution ($\bar{r}_w/\bar{r}_n = 2$), the virtual gelation dose, D_{vg}, is related to the measured gelation dose by the approximate equation[47]

$$D_{vg} = D_g\left[1 - \frac{1}{3}\frac{\beta}{\alpha}\frac{\bar{r}_n}{\bar{r}_w}\right] \quad \text{(B1)}$$

The virtual dose is the gelation dose which would have been observed if chain scission were absent. The ratio β/α is determined by extrapolating a Charlesby–Pinner plot to infinite dose ($1/D \rightarrow 0$). D_g is also obtained graphically,[48] for example, by extrapolating a plot of the gel content vs. dose to zero gel. D_{vg} is then calculated from eq B1 and used to obtain the cross-linking rate by

$$\alpha_0 = 1/D_{vg}\bar{r}_w \quad \text{(B2)}$$

When these equations were used to calculate α_0 and β_0 for our polymers, the values were within 1% of those determined by the nonlinear regression analysis.

The equations for calculating the gel content and the network structure have limiting forms at high cross-link densities ($\gamma \gg 1$) which are much simpler than the general relations, eq 14, 21, and 22. We find[29]

$$g = 2\lambda(1 - 1/\gamma\xi) - \lambda^2(1 - 2/\gamma\xi) \quad \text{(B3)}$$

$$p_1 = 2\lambda(1 - 1/\gamma\xi) - 2\lambda^2(1 - 2/\gamma\xi) \quad \text{(B4)}$$

$$p_2 = \lambda^2(1 - 1/\gamma\xi) \quad \text{(B5)}$$

where $\xi = \beta/\alpha + g$, $\lambda = g/\xi$, and $\gamma = \alpha\bar{r}_n$. At high cross-link densities g as it appears in λ and on the right-hand side of eq B3–B5 can be replaced by $g_{max} = {}^1/_2[1 - 2\beta/\alpha + (1 + 4\beta/\alpha)^{1/2}]$. The gel fraction and the network structure are now explicit functions of two parameters: γ, the number of cross-linked units per molecule, and β/α, the ratio of scissions to cross-linked units. To judge the accuracy of eq B5, the trapping factor was recalculated for the four samples of EP 310 listed in Table II. The difference between the two methods varied from 0.3 to 0.6%.

References and Notes

(1) P. J. Flory, "Principles of Polymer Chemistry", Cornell University Press, Ithaca, NY, 1953.
(2) G. Jannink et al., *Macromolecules*, **8**, 804 (1975).
(3) S. F. Edwards, *J. Phys. Soc. Jpn., Suppl.*, **16**, 15 (1969).
(4) L. M. Dossin and W. W. Graessley, *Macromolecules*, **12**, 123 (1979).
(5) N. R. Langley and K. E. Polmanteer, *J. Polym. Sci., Polym. Phys. Ed.*, **12**, 1023 (1974).
(6) E. M. Valles and C. W. Macosko, *Rubber Chem. Technol.*, **49**, 1232 (1976).
(7) J. E. Mark and J. L. Sullivan, *J. Chem. Phys.*, **66**, 1006 (1977).
(8) J. E. Mark, R. R. Rahalkar, and J. L. Sullivan, *J. Chem. Phys.*, **70**, 1794 (1979).
(9) K. J. Smith, Jr., and R. J. Gaylord, *J. Polym. Sci., Polym. Phys. Ed.*, **13**, 2069 (1975).
(10) P. J. Flory, *Proc. R. Soc. London, Ser. A*, **351**, 351 (1976).
(11) J. Scanlan, *J. Polym. Sci.*, **43**, 510 (1960).
(12) L. Case, *J. Polym. Sci.*, **45**, 397 (1960).
(13) G. Ronca and G. Allegra, *J. Chem. Phys.*, **63**, 4990 (1975).
(14) P. J. Flory, *J. Chem. Phys.*, **12**, 5720 (1977).
(15) N. R. Langley, *Macromolecules*, **1**, 348 (1968).
(16) D. S. Pearson and W. W. Graessley, *Macromolecules*, **11**, 528 (1978).
(17) M. Doi and S. F. Edwards, *J. Chem. Soc., Faraday Trans. 2*, **74**, 1789, 1802, 1818 (1978).
(18) W. W. Graessley, *J. Polym. Sci., Polym. Phys. Ed.*, **18**, 27 (1980).
(19) W. S. Park, Doctoral Dissertation, Northwestern University, 1978.
(20) S. Grubisie, P. Rempp, and H. Benoit, *J. Polym. Sci., Polym. Lett. Ed.*, **5**, 753 (1967).
(21) W. V. Smith, *J. Appl. Polym. Sci.*, **18**, 3685 (1976).
(22) W. S. Park and W. W. Graessley, *J. Polym. Sci., Polym. Phys. Ed.*, **15**, 71, 85 (1977).
(23) G. Ver Strate, private communication.
(24) G. Ver Strate, to be submitted for publication.
(25) R. J. Raju et al., *J. Polym. Sci., Polym. Phys. Ed.*, **17**, 1183 (1979).
(26) J. D. Ferry, "Viscoelastic Properties of Polymers", 2nd ed., Wiley, New York, 1970.
(27) J. R. Richards, R. G. Mancke, and J. D. Ferry, *J. Polym. Sci., Polym. Lett. Ed.*, **2**, 197 (1964).
(28) L. V. Spencer, *NBS Monogr.*, 1 (1959).

(29) D. S. Pearson, Doctoral Dissertation, Northwestern University, 1978.
(30) L. H. Tung in "Polymer Fractionation", M. J. R. Cantow, Ed., Academic Press, New York, 1967, pp 380–414.
(31) A. Charlesby, "Atomic Radiation and Polymers", Pergammon Press, New York, 1960.
(32) J. E. Mark, *Rubber Chem. Technol.*, **46**, 593 (1973).
(33) G. Natta, G. Crespi, and V. Flisi, *J. Polym. Sci., Polym. Chem. Ed.*, **1**, 3569 (1963).
(34) J. A. Barrie and J. Standen, *Polymer*, **8**, 97 (1967).
(35) V. Flisi, G. Crespi, and A. Valvasorri, *Rubber Chem. Technol.*, **43**, 778 (1970).
(36) A. Romanov and V. Pollak, *J. Polym. Sci., Polym. Phys. Ed.*, **8**, 1879 (1970).
(37) S. Bruckner et al., *Eur. Polym. J.*, **10**, 347 (1974).
(38) J. E. Mark, *J. Chem. Phys.*, **57**, 2541 (1972).
(39) C. K. Shih and E. F. Cluff, *J. Appl. Polym. Sci.*, **21**, 2885 (1977).
(40) J. E. Mark, *Rubber Chem. Technol.*, **48**, 495 (1975).
(41) J. D. Ferry and H. Kan, *Rubber Chem. Technol.*, **51**, 731 (1978).
(42) F. F. Rieke and W. Prepejchal, *Phys. Rev. A*, **6**, 1507 (1972).
(43) M. J. Berger and S. M. Seltzer, "Tables of Energy Losses and Ranges of Electrons and Positrons", NASA Publication N65-12506, Clearinghouse for Federal Scientific and Technical Information, Springfield, VA, 1964.
(44) E. Merzbacher, "Quantum Mechanics", 2nd ed., Wiley, New York, 1970.
(45) J. R. Falender, G. S. Yeh, and J. E. Mark, *J. Chem. Phys.*, **70**, 5324 (1979).
(46) L. M. Alberino and W. W. Graessley, *J. Phys. Chem.*, **72**, 4229 (1968).
(47) W. W. Graessley, *J. Phys. Chem.*, **68**, 2258 (1964).
(48) D. S. Pearson, B. J. Skutnik, and G. G. A. Böhm, *J. Polym. Sci., Polym. Phys. Ed.*, **12**, 925 (1974).

Kinetics of Polycondensation and Copolycondensation by Ester-Interchange Reactions

Man Jung Han

Department of Chemical Engineering, Ajou Institute of Technology, Suweon, 170 South Korea. *Received September 28, 1979*

ABSTRACT: The kinetics of polycondensation and copolycondensation by ester-interchange reactions were investigated by using 2-hydroxyethyl terephthalate and 2-hydroxy-*n*-propyl terephthalate as monomers. It was found that the polycondensation of diol esters of dibasic acids followed second-order kinetics with respect to the concentrations of hydroxyl and ester groups in the monomers. New equations for calculation of the rate constants of cross reactions and of the composition ratios in the copolymer were derived. The reactivity ratios of the copolycondensations and the azeotropic composition were calculated on the basis of the rate constants. The composition diagram of the copolycondensation was obtained.

Hydroxyl-terminated aliphatic polyesters are important materials in the production of the polyurethane used in several fields as a thermoplastic elastomer. As is well-known, the polyester segments build the soft blocks in the polyurethane and the variation of the polyester composition changes the physical properties of the polyurethane. The variables in the polyester composition are the dibasic acids (succinic, glutaric, adipic, azelaic acids) and the diols (ethanediol, 1,2-propanediol, 1,4-butanediol, 1,6-hexanediol).

The urethane polymer formation is most easily controlled when the polyester contains only hydroxyl groups as reactive sites. Hence the preferred polyesters have been those with very low acid end groups and very low water content. In order to minimize the acid end groups and water content, laboratory and industrial syntheses have often involved ester-interchange reactions of the diol esters of dibasic acids.

Unlike polyesterification reactions of dibasic acids and diols, which have been studied in many laboratories,[1-5] studies on polycondensation of diol esters of dibasic acids by ester-interchange reactions are scarce. In this paper we report the kinetics of the polycondensation and copolycondensation of diol esters or dibasic acids by ester-interchange reactions.

Kinetics

Polycondensation. The polycondensation of the diol ester of a dibasic acid can be expressed generally as

$$2\text{HOROOCR'COOROH} \xrightarrow{k} \text{HOROOCR'COOROOCR'COOROH} + \text{HOROH} \quad (1)$$

If the concentration of the hydroxyl group is [OH] and the concentration of the ester group is [COO] and if the diols formed during the reaction are continuously removed and no catalyst is used, the kinetics of the polycondensation can be written as

$$-\mathrm{d[OH]}/\mathrm{d}t = k[\mathrm{OH}][\mathrm{COO}] \quad (2)$$

At the initial stage of the polycondensation the concentrations of hydroxyl and ester groups are equal; we obtain therefore second-order kinetics

$$-\mathrm{d[OH]}/\mathrm{d}t = k[\mathrm{OH}]^2 \quad (3)$$

Rearrangement and integration of the equation gives eq 4. A plot of $1/[\mathrm{OH}]$ vs. time yields the rate constant of the polycondensation.

$$1/[\mathrm{OH}] = kt + C \quad (4)$$

Copolycondensation. The copolycondensation of two different diol esters of dibasic acids for conditions where the hydroxyl group of the second chain end attacks the ester group of the first chain end can be written as the sequence of reactions in eq 5–8. Reactions 6 and 7 are

$$\text{---RCOOR}_1\text{OH} + \text{HOR}_1\text{OOCR---} \xrightarrow{k_{11}} \text{---RCOOR}_1\text{OOCR---} + \text{HOR}_1\text{OH} \quad (5)$$

$$\text{---RCOOR}_1\text{OH} + \text{HOR}_2\text{OOCR---} \xrightarrow{k_{12}} \text{---RCOOR}_2\text{OOCR---} + \text{HOR}_1\text{OH} \quad (6)$$

$$\text{---RCOOR}_2\text{OH} + \text{HOR}_1\text{OOCR---} \xrightarrow{k_{21}} \text{---RCOOR}_1\text{OOCR---} + \text{HOR}_2\text{OH} \quad (7)$$

0024-9297/80/2213-1009$01.00/0